Dimensionality of excitons in stacked van der Waals materials: The example of hexagonal boron nitride

Wahib Aggoune,[1,2] Caterina Cocchi,[1,3,*] Dmitrii Nabok,[1,3] Karim Rezouali,[2] Mohamed Akli Belkhir,[2] and Claudia Draxl[1,3,†]

[1]*Institut für Physik and IRIS Adlershof, Humboldt-Universität zu Berlin, Berlin, Germany*
[2]*Laboratoire de Physique Théorique, Faculté des Sciences Exactes, Université de Bejaia, 06000 Bejaia, Algeria*
[3]*European Theoretical Spectroscopic Facility (ETSF)*

With the example of hexagonal boron nitride, we demonstrate how the character of electron-hole (*e-h*) pairs in van der Waals bound low-dimensional systems is driven by layer stacking. Four types of excitons appear, with either a two- or three-dimensional spatial extension. Electron and hole distributions are either overlapping or exhibit a charge-transfer nature. We discuss under which structural and symmetry conditions they appear and they are either dark or bright. This analysis provides the key elements to identify, predict, and possibly tailor the character of *e-h* pairs in van der Waals materials.

Two-dimensional (2D) systems and layered weakly bound structures thereof are considered the materials of the 21st century. Their wealth of intriguing properties is widely explored from a fundamental scientific point of view but also in view of a plethora of possible applications [1,2]. Hexagonal boron nitride (h-BN) is one of these materials, consisting of covalently bound sheets that are held together by van der Waals (vdW) forces [3]. h-BN is a wide-gap semiconductor, exhibiting pronounced excitonic effects in its optical excitations that are present irrespective of the material's dimensionality [4–11]. Owing to the flat geometry of its in-plane hexagonal lattice, h-BN is often chosen as a building block in vdW heterostructures [12–15]. Combining different 2D systems, quantum confinement effects allow for tailoring their optoelectronic properties [16–18]. This not only concerns level alignment at the interface [19–26] but also the way the system interacts with light, i.e., quantum efficiency, as well as the character and spatial distribution of electron-hole (*e-h*) pairs [14,15,27–32].

In this Rapid Communication, we show that the nature and dimensionality of excitons can also be governed in a single vdW bound bulk material, taking h-BN as an example. This seems surprising at a first glance as *e-h* pairs in this material have been found to exhibit basically the same character and extension in bulk [6–8], monolayers [10], as well as in interfaces with graphene [14]. Here, we demonstrate how strongly stacking impacts the optical excitations of a vdW crystal at the onset of absorption and beyond. By varying the arrangement of individual h-BN layers, we find in total four types of electron-hole pairs, of a two-dimensional, three-dimensional (3D), and charge-transfer character, and discuss their appearance by symmetry considerations. We focus on the five structures that are obtained by including four inequivalent atoms in the unit cell, allowing only a rigid translation by one bond length and/or exchanged positions between the two

atomic species. We employ density functional theory [33–37] and many-body perturbation theory (MBPT, including $G_0 W_0$ [38,39] and the Bethe-Salpeter equation [40–43]), implemented in the all-electron framework of the exciting code [44–46].

Prototypes of the four kinds of excitations that can appear in h-BN are displayed in Fig. 1. There, the electronic distribution surrounding a fixed position of the hole is plotted. The first type is a 2D exciton, i.e., with the electron and hole on the same layer. Such *e-h* pairs are typical of atomically thin sheets [10], but may also dominate the onset of absorption in multilayer crystals [6–8,25,48]. We notice that these excitons are very localized, extending only up to three lattice parameters in the in-plane direction. The trigonal shape of the excitonic wave function reflects the hexagonal symmetry of the monolayer. As extensively discussed in earlier works on h-BN based on MBPT [6,7], this exciton is twofold degenerate, and its shape results from the averaged densities of the two degenerate contributions [7].

In multilayer structures, *e-h* pairs can also be extended in the vertical direction, with the electron and/or the hole spreading over neighboring layers. This is the case of *charge-transfer* (CT) excitons, where the electron and the hole sit on different layers and their extension is limited to a few (here up to five) lattice parameters in the in-plane direction. Viewed from the top, this *e-h* pair also exhibits clear trigonal symmetry (see Fig. 1). CT excitons are particularly intriguing in view of generating photocurrents [28,49] or, if characterized by large binding energies, even Bose-Einstein condensates [50–54].

The other two types of excitons shown in Fig. 1 exhibit a 3D distribution that can be either localized in the in-plane direction (3D-*l*) or delocalized over the whole space (3D-*d*). In both cases, the electron distribution overlaps with the hole distribution and further extends uniformly and symmetrically to the adjacent layers. In the 3D-*l e-h* pairs, the electron probability density is significantly enhanced in the layer where the hole resides. This *e-h* pair exhibits a trigonal in-plane shape with an extension similar to the one of 2D excitons. In

*Corresponding author: caterina.cocchi@physik.hu-berlin.de
†Corresponding author: claudia.draxl@physik.hu-berlin.de
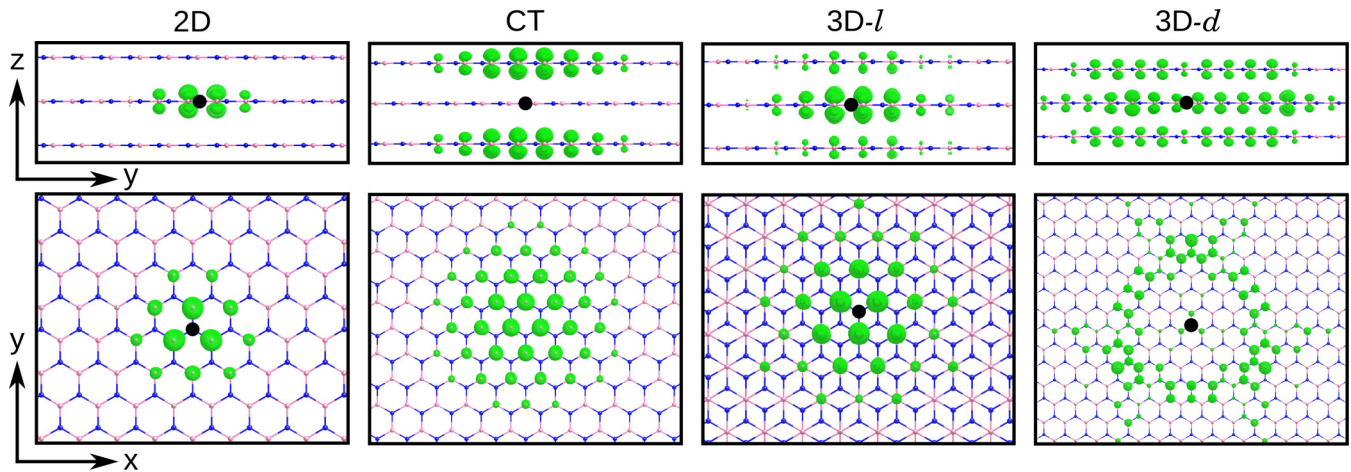
241114-1

FIG. 1. Real-space distribution (side and top view) of the four types of excitons that can appear in bulk h-BN upon different layer stackings. From left to right: 2D exciton, with the electron and the hole sitting on the same layer; charge-transfer (CT) exciton, with the electron and the hole on different layers; 3D exciton with localized (3D-*l*) and delocalized (3D-*d*) in-plane extension. The hole is indicated by the black dot and the electron distribution by the green isosurface. B atoms are pink and N atoms blue. Figures produced with the VESTA software [47].

addition to the specific arrangement of the atoms, as discussed in the following, the 3D-*l* excitons appear in configurations where the neighboring layers are linked by inversion symmetry. 3D-*d* excitons appear above the onset of absorption and are characterized by a delocalized spatial distribution in the three directions. In the h-BN structures considered here, these *e*-*h* pairs extend up to 12 lattice parameters in the in-plane directions and across three layers in the stacking direction [55]. While reflecting a resonant character and reduced crystal symmetry, such excitons exhibit a trigonal shape, typical of higher-energy excitons in monolayer h-BN [10].

In order to relate the exciton characters described above with symmetry and atomic arrangement of the considered stackings, it is instructive to inspect more closely the corresponding geometries [55–57] and analyze their electronic structure and optical spectra. In the simplest configuration, all atoms of the two inequivalent layers are aligned on top of each other (*AA* stacking). In the *AB* or Bernal stacking, every second atom lies on the *hollow* site. These patterns, initially defined for monatomic stacks of graphitic layers [58], can be further modulated by the positions of the two atomic species. The *AA* configuration results in the *AA'* stacking [59] if B and N atoms of alternating layers lie on top of each other. We note in passing that this is considered to be the most stable h-BN arrangement [3,60,61]. The *A'B* and *AB'* stackings are obtained from the *AB* configuration: Instead of alternating B and N atoms on the *hollow* site, as in the *AB* pattern, in the *A'B* (*AB'*) arrangement, only N (B) atoms occupy the *hollow* position. While *AB* configuration has been reported for bilayer structures [62], other arrangements are observed only locally in few-layer stacks [63–67]. Complex modulated patterns have been achieved in combination with graphene [68–73] while transitions from a stacking sequence to another one have been shown upon morphological deformation [9]. These different layer stackings combined with atomic arrangements in the vertical direction strongly impact the electronic structure (Fig. 2, right panel) and the optical spectra accordingly. In the following, we discuss how this structure-property relation determines the conditions under which different types of *e*-*h* pairs are formed.

Alternative approaches to extract this information are based on model Hamiltonians [10,74,75], analytic envelope-function modeling [76], and double-Bader analysis [77].

In Fig. 2 we display the optical spectra (left panel) together with the quasiparticle (QP) band structures (right panel). Our results are in good agreement with available experimental data for the *AA'* stacking [78–86] (see also Ref. [55]). First, we consider the character of the first bright exciton in each configuration (green bars). The contributions of individual electronic states to the *e*-*h* pairs are indicated by the green circles drawn on top of the QP band structures [55]. Regardless of the stacking, the direct QP gap of bulk h-BN is always along or in the vicinity of the *K*-*H* path in the Brillouin zone (BZ). Hence, all excitations comprised within the first peak and up to ~1 eV above it always stem from transitions between QP states in the gap region. The two uppermost valence bands (VB, VB-1) and the two lowest conduction bands (CB, CB+1) are energetically very close to each other, due to the presence of two atoms of the same species in the unit cell. These bands have a well-defined N and B character (highlighted in color in Fig. 2), which is related to the atomic structure of the constituting species and thus independent of the layer stacking.

The first bright *e*-*h* pair has a 2D character in the *AA'*, *AA*, and *AB* configurations. In the *AA'* stacking, it is twofold degenerate, owing to the symmetry of the lattice. Due to the parity of the exciton with respect to the inversion symmetry of the crystal, a doubly degenerate dark exciton with 2D distribution appears lowest in energy (here, at 5.50 eV; for a comparison with experiments, see Ref. [55]). These findings are in agreement with earlier studies of this h-BN phase [7,75,87]. The 2D character of the first bright exciton is closely related to the electronic structure of the corresponding arrangement. In the *AA'* and *AB* stackings, where atoms of the same species never lie on top of each other, VB-1 and VB (and likewise CB and CB+1) are (almost) degenerate along the entire *K*-*H* path, as reported also in Refs. [6,60,88,89]. At the high-symmetry point *H* the Kohn-Sham wave functions sit on one inequivalent layer only. In the *AB* configuration the same behavior is found also at *K*, with the consequence that in this
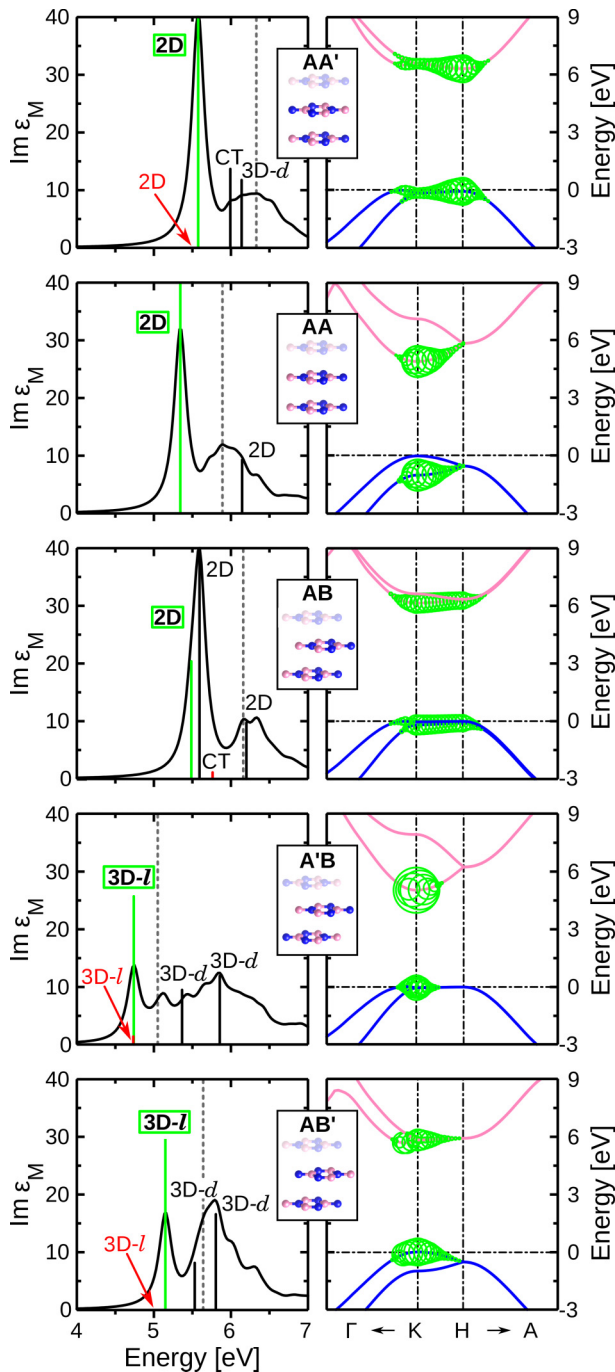
FIG. 2. Left: Optical absorption spectra, given by the imaginary part of the macroscopic dielectric function, of the five considered stacking arrangements of h-BN (insets). The character of selected excitations is indicated following the nomenclature in Fig. 1. The height of the vertical bars is indicative of their relative intensity [55]. The first bright exciton is marked by a green bar with the corresponding label framed in green. Dark excitons at lowest energies are indicated by red arrows. A Lorentzian broadening of 0.1 eV is applied to all spectra. Direct QP gaps are marked by dashed gray lines. Right: Reciprocal-space distribution of the first bright exciton with band character highlighted in color: blue for N and pink for B. The sizes of the green circles indicate the **k**-resolved band contributions to the corresponding excitation (green bar) [55]. Fermi energy set to zero at the valence band maximum and marked by a dashed-dotted line.

stacking the hole and the electron of the 2D exciton are always localized within one specific h-BN sheet. Conversely, in the AA' and AA arrangements, electronic wave functions tend to be delocalized over all layers towards the high-symmetry point K. As a result, the 2D exciton appears with the same probability in any layer [55,90].

The lowest-energy exciton is optically allowed in those stackings that lack inversion symmetry between the layers. This is the case of the AB arrangement, where the absence of inversion symmetry allows for the presence of two optically active e-h pairs, both twofold degenerate and encompassed within the first peak (see Fig. 2). Likewise, in the AA stacking the lowest-energy exciton is optically allowed and bears a 2D distribution. It dominates the onset of absorption, giving rise to a sharp peak. Conversely, in the AA' stacking, exhibiting inversion symmetry, the first exciton is dark. Overall, the spectra of these three structures look quite similar: They are characterized by an intense excitonic peak around 5.5 eV, followed by a broader and less intense hump at higher energies. The binding energy of the first optically active exciton ranges between 0.50 and 0.75 eV, depending on the specific structure [55]. We define the binding energy as the difference between the excitation energy computed with the e-h interaction included (by solving the Bethe-Salpeter equation) and neglected (independent QP approximation) [55]. This definition is general and holds for any excitation independent of its position in the spectrum. For the first bright excitons discussed above, it coincides with the often adopted definition of binding energy as the difference between fundamental and optical gaps.

In the $A'B$ and AB' configurations the lowest-energy bright exciton has a 3D-l nature. This e-h pair has the same in-plane extension as the 2D one, but the electron is vertically spread over two neighboring layers to the one hosting the hole. This distribution can be once again traced back to the symmetry and character of the electronic states near the gap that contribute to it. As discussed above, in the $A'B$ (AB') stackings, layers are staggered with B (N) atoms vertically aligned on top of each other. This makes the CB (VB) energetically split from the CB+1 (VB-1). The wave functions of these bands along the K-H path are therefore delocalized within all layers [55]. Under these conditions, the resulting e-h pairs extend to the neighboring layers.

The inversion symmetry in these structures is responsible for the presence of a forbidden exciton that is lowest in energy: In the $A'B$ lattice, the first dark e-h pair has the same energy as the first bright 3D-l exciton, while in the AB' stacking it is found at approximately 5 eV. The intensity of the first peak is considerably lower compared to the other arrangements, due to the reduced wave-function overlap between the QP states contributing to it. In the $A'B$ arrangement, the direct QP gap and thus the onset of absorption are significantly redshifted compared to the AA' stacking, up to 1.3 and 0.8 eV, respectively. Depending on the stacking arrangement, only 2D or 3D-l excitons can appear at the onset of absorption and are always associated with intense peaks. Their oscillator strength is related to the symmetry conditions as well as to the large overlap between the π/π^* wave functions of the bands involved in the corresponding transitions. Their spatial localization, in turn, reflects the bound character of these e-h pairs. On the other hand, CT and 3D-d e-h pairs emerge

only at higher energies and, especially the former, upon strict symmetry and structural requirements, reflecting the layer-selective distribution of the contributing bands. In fact, CT excitons can appear only in the AA' and AB stackings, since in these structures the condition that atoms of the same species are aligned on top of each other is never satisfied. In the AA' arrangement, the CT exciton marked in the spectrum of Fig. 2 originates from transitions between the VB-1 and the CB+1, and between the VB and the CB, at the H point in the BZ. Here, these bands are degenerate and the corresponding electronic wave functions are spread over N and B atoms belonging to different h-BN layers. The CT exciton is dipole allowed only in the out-of-plane polarization direction and does not exhibit any degeneracy. As a result, the in-plane distribution of this e-h pair differs from the one shown in Fig. 1 [55]. In the spectrum of the AB arrangement, we find a doubly degenerate CT exciton with in-plane polarization, stemming from transitions between the VB and the CB in the vicinity of the K point. According to the wave-function distribution of these bands, the hole and the electron sit on different layers, giving rise to the CT character of this exciton. Its weak oscillator strength is due to the small overlap between the electron and hole wave functions [55].

Delocalized 3D excitons characterize mainly the high-energy window of the optical spectra. They only appear when inversion symmetry is present. In the AA' configuration the 3D-d exciton marked above 6 eV is twofold degenerate and has a binding energy of 0.2 eV. Viewed from the side (Fig. 1), this type of exciton extends symmetrically to the nearest-neighboring layers in the vertical direction. This in-plane distribution appears in the h-BN monolayer [10] and is apparently preserved also in multilayer structures. Also in the $A'B$ and AB' configurations, 3D-d excitons are present in the high-energy range, but they exhibit a different in-plane distribution that reflects the structural arrangement [55]. It is worth noting that in the AA and AB configurations, where inversion symmetry is absent, delocalized 2D excitons with a trigonal shape appear in the high-energy range. Remarkably, they resemble higher-energy excitons in monolayer h-BN [10,55].

Finally, above 1 eV from the onset of absorption of each stacking, very delocalized excitations appear (not shown; see also Ref. [55]). They stem from a number of mixed transitions between electronic states far from the QP gap and do not correspond to any type of exciton depicted in Fig. 1. Due to their resonant character of band-to-band transitions, their

delocalized distribution resembles that of Kohn-Sham states. Such 3D excitations with an extremely extended character are expected to form more favorably in vdW crystals and heterostructures exhibiting superlattices and/or Moiré patterns. These complex structural arrangements, which are observed in realistic samples (see, e.g., Refs. [91–93] for graphene/h-BN interfaces), tend to decrease the symmetry of the system, thereby promoting weakly bound e-h pairs.

The general arguments underpinning the presented analysis can be directly extended to other vdW materials. While group-IV monatomic layers (graphene, silicene, etc.) exhibit a semimetallic character [94,95], binary compounds such as transition-metal dichalcogenides have a pronounced excitonic behavior largely influenced by layer stacking [74,96–106]. Spin-orbit coupling [107–109] and an indirect-direct band-gap transition upon an increasing number of layers [110,111] further enrich their excited-state properties. Also group-V vdW materials, such as phosphorene, are known for the dependence of their gap on the number of layers and the stacking order [112–119]. Layer displacement in these cases can evidently further contribute to tune the character of the e-h pairs.

In summary, we have analyzed the four types of excitations that appear in different stacking arrangements of bulk h-BN, considered here as a prototypical vdW material. We have shown that localized e-h pairs with a purely 2D character appear in all configurations. Charge-transfer excitons occur only if specific structural and symmetry conditions are fulfilled. 3D excitons with a more or less extended spatial distribution are also present at the onset of absorption and/or above it, depending on the layer stacking. Our results demonstrate the interplay between structural arrangements and optical properties in stacked vdW materials, providing the key elements to assess, foresee, and tune the character of their e-h pairs. As such, our findings contribute to the fascinating perspectives of designing vdW heterostructures with customized characteristics, achieved through a controlled modulation of the electronic structure via layer patterning.

Input and output files of our calculations can be downloaded free of charge from the NOMAD repository [120].

[1] G. Bhimanapati, Z. Lin, V. Meunier, Y. Jung, J. Cha, S. Das, D. Xiao, Y. Son, M. Strano, V. Cooper *et al.*, ACS Nano **9**, 11509 (2015).

[2] C. Tan, X. Cao, X.-J. Wu, Q. He, J. Yang, X. Zhang, J. Chen, W. Zhao, S. Han, G.-H. Nam *et al.*, Chem. Rev. **117**, 6225 (2017).

[3] R. S. Pease, Nature (London) **165**, 722 (1950).

[4] K. Watanabe, T. Taniguchi, and H. Kanda, Nat. Mater. **3**, 404 (2004).

[5] Y. Kubota, K. Watanabe, O. Tsuda, and T. Taniguchi, Science **317**, 932 (2007).

[6] B. Arnaud, S. Lebegue, P. Rabiller, and M. Alouani, Phys. Rev. Lett. **96**, 026402 (2006).

[7] L. Wirtz, A. Marini, M. Grüning, C. Attaccalite, G. Kresse, and A. Rubio, Phys. Rev. Lett. **100**, 189701 (2008).

[8] S. Galambosi, L. Wirtz, J. A. Soininen, J. Serrano, A. Marini, K. Watanabe, T. Taniguchi, S. Huotari, A. Rubio, and K. Hämäläinen, Phys. Rev. B **83**, 081413(R) (2011).

[9] R. Bourrellier, M. Amato, L. H. Galvão Tizei, C. Giorgetti, A. Gloter, M. I. Heggie, K. March, O. Stéphan, L. Reining, M. Kociak *et al.*, ACS Photonics **1**, 857 (2014).

[10] T. Galvani, F. Paleari, H. P. C. Miranda, A. Molina-Sánchez, L. Wirtz, S. Latil, H. Amara, and F. Ducastelle, Phys. Rev. B **94**, 125303 (2016).

[11] J. Koskelo, G. Fugallo, M. Hakala, M. Gatti, F. Sottile, and P. Cudazzo, Phys. Rev. B **95**, 035125 (2017).

[12] C. R. Dean, A. F. Young, I. Meric, C. Lee, L. Wang, S. Sorgenfrei, K. Watanabe, T. Taniguchi, P. Kim, K. Shepard *et al.*, Nat. Nanotechnol. **5**, 722 (2010).

[13] J. Yan, K. W. Jacobsen, and K. S. Thygesen, Phys. Rev. B **86**, 045208 (2012).

[14] W. Aggoune, C. Cocchi, D. Nabok, K. Rezouali, M. A. Belkhir, and C. Draxl, J. Phys. Chem. Lett. **8**, 1464 (2017).

[15] S. Latini, K. T. Winther, T. Olsen, and K. S. Thygesen, Nano Lett. **17**, 938 (2017).

[16] A. K. Geim and I. V. Grigorieva, Nature (London) **499**, 419 (2013).

[17] K. Novoselov, A. Mishchenko, A. Carvalho, and A. C. Neto, Science **353**, aac9439 (2016).

[18] D. Jariwala, T. J. Marks, and M. C. Hersam, Nat. Mater. **16**, 170 (2017).

[19] J. Kang, S. Tongay, J. Zhou, J. Li, and J. Wu, Appl. Phys. Lett. **102**, 012111 (2013).

[20] M.-H. Chiu, C. Zhang, H.-W. Shiu, C.-P. Chuu, C.-H. Chen, C.-Y. S. Chang, C.-H. Chen, M.-Y. Chou, C.-K. Shih, and L.-J. Li, Nat. Commun. **6**, 7666 (2015).

[21] V. O. Özçelik, J. G. Azadani, C. Yang, S. J. Koester, and T. Low, Phys. Rev. B **94**, 035125 (2016).

[22] Q. Fu, D. Nabok, and C. Draxl, J. Phys. Chem. C **120**, 11671 (2016).

[23] Y. Guo and J. Robertson, Appl. Phys. Lett. **108**, 233104 (2016).

[24] C. Zhang, C. Gong, Y. Nie, K.-A. Min, C. Liang, Y. J. Oh, H. Zhang, W. Wang, S. Hong, L. Colombo *et al.*, 2D Mater. **4**, 015026 (2016).

[25] K. S. Thygesen, 2D Mater. **4**, 022004 (2017).

[26] Q. Fu, C. Cocchi, D. Nabok, A. Gulans, and C. Draxl, Phys. Chem. Chem. Phys. **19**, 6196 (2017).

[27] M. Milko, P. Puschnig, P. Blondeau, E. Menna, J. Gao, M. A. Loi, and C. Draxl, J. Phys. Chem. Lett. **4**, 2664 (2013).

[28] X. Hong, J. Kim, S.-F. Shi, Y. Zhang, C. Jin, Y. Sun, S. Tongay, J. Wu, Y. Zhang, and F. Wang, Nat. Nanotechnol. **9**, 682 (2014).

[29] F. Ceballos, M. Z. Bellus, H.-Y. Chiu, and H. Zhao, ACS Nano **8**, 12717 (2014).

[30] L. Li, R. Long, and O. V. Prezhdo, Chem. Mater. **29**, 2466 (2016).

[31] M. Baranowski, A. Surrente, L. Klopotowski, J. Urban, N. Zhang, D. K. Maude, K. Wiwatowski, S. Mackowski, Y.-C. Kung, D. Dumcenco *et al.*, Nano Lett. **17**, 6360 (2017).

[32] Z. Guan, C.-S. Lian, S. Hu, S. Ni, J. Li, and W. Duan, J. Phys. Chem. C **121**, 3654 (2017).

[33] P. Hohenberg and W. Kohn, Phys. Rev. **136**, B864 (1964).

[34] W. Kohn and L. J. Sham, Phys. Rev. **140**, A1133 (1965).

[35] J. P. Perdew, K. Burke, and M. Ernzerhof, Phys. Rev. Lett. **77**, 3865 (1996).

[36] A. Tkatchenko and M. Scheffler, Phys. Rev. Lett. **102**, 073005 (2009).

[37] S. Grimme, J. Comput. Chem. **27**, 1787 (2006).

[38] L. Hedin, Phys. Rev. **139**, A796 (1965).

[39] M. S. Hybertsen and S. G. Louie, Phys. Rev. Lett. **55**, 1418 (1985).

[40] W. Hanke and L. J. Sham, Phys. Rev. B **21**, 4656 (1980).

[41] G. Strinati, Riv. Nuovo Cimento **11**, 1 (1988).

[42] M. Rohlfing and S. G. Louie, Phys. Rev. B **62**, 4927 (2000).

[43] P. Puschnig and C. Ambrosch-Draxl, Phys. Rev. B **66**, 165105 (2002).

[44] A. Gulans, S. Kontur, C. Meisenbichler, D. Nabok, P. Pavone, S. Rigamonti, S. Sagmeister, U. Werner, and C. Draxl, J. Phys.: Condens. Matter. **26**, 363202 (2014).

[45] S. Sagmeister and C. Ambrosch-Draxl, Phys. Chem. Chem. Phys. **11**, 4451 (2009).

[46] D. Nabok, A. Gulans, and C. Draxl, Phys. Rev. B **94**, 035118 (2016).

[47] K. Momma and F. Izumi, J. Appl. Crystallogr. **44**, 1272 (2011).

[48] A. Molina-Sánchez, K. Hummer, and L. Wirtz, Surf. Sci. Rep. **70**, 554 (2015).

[49] C. Deibel, T. Strobel, and V. Dyakonov, Adv. Mater. **22**, 4097 (2010).

[50] H. Min, R. Bistritzer, J.-J. Su, and A. H. MacDonald, Phys. Rev. B **78**, 121401(R) (2008).

[51] M. Y. Kharitonov and K. B. Efetov, Phys. Rev. B **78**, 241401 (2008).

[52] P. Cudazzo, C. Attacalite, I. V. Tokatly, and A. Rubio, Phys. Rev. Lett. **104**, 226804 (2010).

[53] A. Perali, D. Neilson, and A. R. Hamilton, Phys. Rev. Lett. **110**, 146803 (2013).

[54] M. Fogler, L. Butov, and K. Novoselov, Nat. Commun. **5**, 4555 (2014).

[55] See Supplemental Material at http://link.aps.org/supplemental/10.1103/PhysRevB.97.241114 for computational details and as well as additional information about the structural, electronic, and optical properties of all considered stackings, including comparisons with experiments, when available, which includes Refs. [3,6,7,9,10,35–41,44–47,56,57,59–67,75,78–89].

[56] N. Marom, J. Bernstein, J. Garel, A. Tkatchenko, E. Joselevich, L. Kronik, and O. Hod, Phys. Rev. Lett. **105**, 046801 (2010).

[57] O. Hod, J. Chem. Theory Comput. **8**, 1360 (2012).

[58] J. D. Bernal, Proc. R. Soc. London, Ser. A **106**, 749 (1924).

[59] V. Solozhenko, G. Will, and F. Elf, Solid State Commun. **96**, 1 (1995).

[60] L. Liu, Y. P. Feng, and Z. X. Shen, Phys. Rev. B **68**, 104102 (2003).

[61] G. Constantinescu, A. Kuc, and T. Heine, Phys. Rev. Lett. **111**, 036104 (2013).

[62] J. H. Warner, M. H. Rummeli, A. Bachmatiuk, and B. Büchner, ACS Nano **4**, 1299 (2010).

[63] C.-J. Kim, L. Brown, M. W. Graham, R. Hovden, R. W. Havener, P. L. McEuen, D. A. Muller, and J. Park, Nano Lett. **13**, 5660 (2013).

[64] A. Shmeliov, J. S. Kim, K. B. Borisenko, P. Wang, E. Okunishi, M. Shannon, A. I. Kirkland, P. D. Nellist, and V. Nicolosi, Nanoscale **5**, 2290 (2013).

[65] M. H. Khan, G. Casillas, D. R. G. Mitchell, H. K. Liu, L. Jiang, and Z. Huang, Nanoscale **8**, 15926 (2016).

[66] M. H. Khan, H. K. Liu, X. Sun, Y. Yamauchi, Y. Bando, D. Golberg, and Z. Huang, Mater. Today **20**, 611 (2017).

[67] H. Henck, D. Pierucci, Z. Ben Aziza, M. G. Silly, B. Gil, F. Sirotti, G. Cassabois, and A. Ouerghi, Appl. Phys. Lett. **110**, 023101 (2017).

[68] S. M. Kim, A. Hsu, P. Araujo, Y.-H. Lee, T. Palacios, M. Dresselhaus, J.-C. Idrobo, K. K. Kim, and J. Kong, Nano Lett. **13**, 933 (2013).

[69] S. Tang, H. Wang, Y. Zhang, A. Li, H. Xie, X. Liu, L. Liu, T. Li, F. Huang, X. Xie *et al.*, Sci. Rep. **3**, 2666 (2013).

[70] T. Gao, X. Song, H. Du, Y. Nie, Y. Chen, Q. Ji, J. Sun, Y. Yang, Y. Zhang, and Z. Liu, Nat. Commun. **6**, 6835 (2015).

[71] A. Khanaki, H. Tian, Z. Xu, R. Zheng, Y. He, Z. Cui, J. Yang, and J. Liu, Nanotechnology **29**, 035602 (2017).

[72] J. M. Wofford, S. Nakhaie, T. Krause, X. Liu, M. Ramsteiner, M. Hanke, H. Riechert, and J. M. J. Lopes, Sci. Rep. **7**, 43644 (2017).

[73] R. Zheng, A. Khanaki, H. Tian, Y. He, Y. Cui, Z. Xu, and J. Liu, Appl. Phys. Lett. **111**, 011903 (2017).

[74] T. Deilmann and K. S. Thygesen, Nano Lett. **18**, 2984 (2018).

[75] F. Paleari, T. Galvani, H. Amara, F. Ducastelle, A. Molina-Sánchez, and L. Wirtz, arXiv:1803.00982.

[76] A. Arora, M. Drüppel, R. Schmidt, T. Deilmann, R. Schneider, M. R. Molas, P. Marauhn, S. Michaelis de Vasconcellos, M. Potemski, M. Rohlfing *et al.*, Nat. Commun. **8**, 639 (2017).

[77] X. Wang, X. Liu, C. Cook, B. Schatschneider, and N. Marom, J. Chem. Phys. **148**, 184101 (2018).

[78] R. Mamy, J. Thomas, G. Jezequel, and J. Lemonnier, J. Phys. (Paris), Lett. **42**, 473 (1981).

[79] C. Tarrio and S. E. Schnatterly, Phys. Rev. B **40**, 7852 (1989).

[80] V. Solozhenko, A. Lazarenko, J.-P. Petitet, and A. Kanaev, J. Phys. Chem. Solids **62**, 1331 (2001).

[81] D. A. Evans, A. G. McGlynn, B. M. Towlson, M. Gunn, D. Jones, T. E. Jenkins, R. Winter, and N. R. J. Poolton, J. Phys.: Condens. Matter **20**, 075233 (2008).

[82] K. Watanabe and T. Taniguchi, Phys. Rev. B **79**, 193104 (2009).

[83] L. Museur, G. Brasse, A. Pierret, S. Maine, B. Attal-Tretout, F. Ducastelle, A. Loiseau, J. Barjon, K. Watanabe, T. Taniguchi *et al.*, Phys. Status Solidi RRL **5**, 214 (2011).

[84] J. Edgar, T. Hoffman, B. Clubine, M. Currie, X. Du, J. Lin, and H. Jiang, J. Cryst. Growth **403**, 110 (2014).

[85] G. Cassabois, P. Valvin, and B. Gil, Nat. Photonics **10**, 262 (2016).

[86] B. Cunningham, M. Grüning, P. Azarhoosh, D. Pashov, and M. van Schilfgaarde, Phys. Rev. Mater. **2**, 034603 (2018).

[87] N. Berseneva, A. Gulans, A. V. Krasheninnikov, and R. M. Nieminen, Phys. Rev. B **87**, 035404 (2013).

[88] X. Blase, A. Rubio, S. G. Louie, and M. L. Cohen, Phys. Rev. B **51**, 6868 (1995).

[89] S.-P. Gao, Solid State Commun. **152**, 1817 (2012).

[90] For consistency with the other structures, also the *AA* stacking is represented in a unit cell containing two layers. On account of the resulting band folding, the lowest-energy transition between VB and CB is optically forbidden and the first allowed transition is between VB-1 and CB.

[91] M. Yankowitz, J. Xue, D. Cormode, J. D. Sanchez-Yamagishi, K. Watanabe, T. Taniguchi, P. Jarillo-Herrero, P. Jacquod, and B. J. LeRoy, Nat. Phys. **8**, 382 (2012).

[92] C. Woods, L. Britnell, A. Eckmann, R. Ma, J. Lu, H. Guo, X. Lin, G. Yu, Y. Cao, R. Gorbachev *et al.*, Nat. Phys. **10**, 451 (2014).

[93] J. R. Wallbank, M. Mucha-Kruczyński, X. Chen, and V. I. Fal'ko, Ann. Phys. **527**, 359 (2015).

[94] M. Aoki and H. Amawashi, Solid State Commun. **142**, 123 (2007).

[95] Y. Xu, X. Li, and J. Dong, Nanotechnology **21**, 065711 (2010).

[96] J. He, K. Hummer, and C. Franchini, Phys. Rev. B **89**, 075409 (2014).

[97] A. H. Reshak, S. A. Khan, and S. Auluck, RSC Adv. **4**, 11967 (2014).

[98] A. F. Rigosi, H. M. Hill, Y. Li, A. Chernikov, and T. F. Heinz, Nano Lett. **15**, 5033 (2015).

[99] J. Yan, J. Xia, X. Wang, L. Liu, J.-L. Kuo, B. K. Tay, S. Chen, W. Zhou, Z. Liu, and Z. X. Shen, Nano Lett. **15**, 8155 (2015).

[100] H. Zheng, X.-B. Li, N.-K. Chen, S.-Y. Xie, W. Q. Tian, Y. Chen, H. Xia, S. B. Zhang, and H.-B. Sun, Phys. Rev. B **92**, 115307 (2015).

[101] Z. Xu, Y. Li, Z. Liu, and C. Li, Physica E **79**, 198 (2016).

[102] E. M. Alexeev, A. Catanzaro, O. V. Skrypka, P. K. Nayak, S. Ahn, S. Pak, J. Lee, J. I. Sohn, K. S. Novoselov, H. S. Shin *et al.*, Nano Lett. **17**, 5342 (2017).

[103] B. Miller, A. Steinhoff, B. Pano, J. Klein, F. Jahnke, A. Holleitner, and U. Wurstbauer, Nano Lett. **17**, 5229 (2017).

[104] P. K. Nayak, Y. Horbatenko, S. Ahn, G. Kim, J.-U. Lee, K. Y. Ma, A.-R. Jang, H. Lim, D. Kim, S. Ryu *et al.*, ACS Nano **11**, 4041 (2017).

[105] R. Gillen and J. Maultzsch, Phys. Rev. B **97**, 165306 (2018).

[106] E. Torun, A. Molina-Sánchez, H. P. Miranda, and L. Wirtz, arXiv:1803.05483.

[107] D. Xiao, G.-B. Liu, W. Feng, X. Xu, and W. Yao, Phys. Rev. Lett. **108**, 196802 (2012).

[108] A. Molina-Sánchez, D. Sangalli, K. Hummer, A. Marini, and L. Wirtz, Phys. Rev. B **88**, 045412 (2013).

[109] W.-T. Hsu, L.-S. Lu, P.-H. Wu, M.-H. Lee, P.-J. Chen, P.-Y. Wu, Y.-C. Chou, H.-T. Jeng, L.-J. Li, M.-W. Chu *et al.*, Nat. Commun. **9**, 1356 (2018).

[110] K. F. Mak, C. Lee, J. Hone, J. Shan, and T. F. Heinz, Phys. Rev. Lett. **105**, 136805 (2010).

[111] C. Ruppert, O. B. Aslan, and T. F. Heinz, Nano Lett. **14**, 6231 (2014).

[112] J. Dai and X. C. Zeng, J. Phys. Chem. Lett. **5**, 1289 (2014).

[113] S. Lei, H. Wang, L. Huang, Y.-Y. Sun, and S. Zhang, Nano Lett. **16**, 1317 (2016).

[114] P. Kumar, B. S. Bhadoria, S. Kumar, S. Bhowmick, Y. S. Chauhan, and A. Agarwal, Phys. Rev. B **93**, 195428 (2016).

[115] D. S. Koda, F. Bechstedt, M. Marques, and L. K. Teles, J. Phys. Chem. C **121**, 3862 (2017).

[116] H.-F. Lin, L.-M. Liu, and J. Zhao, J. Mater. Chem. C **5**, 2291 (2017).

[117] D. Çakır, C. Sevik, and F. M. Peeters, Phys. Rev. B **92**, 165406 (2015).

[118] D. Kecik, E. Durgun, and S. Ciraci, Phys. Rev. B **94**, 205410 (2016).

[119] Y. Mogulkoc, M. Modarresi, A. Mogulkoc, and Y. Ciftci, Comput. Mater. Sci. **124**, 23 (2016).

[120] http://dx.doi.org/10.17172/NOMAD/2018.06.05-1.